Sherlock, B.; Tsimenidis, C.C.; Neasham, J.A., "Signal and receiver design for low-power acoustic communications using m-ary orthogonal code keying," in *OCEANS 2015 - Genova* , vol., no., pp.1-10, 18-21 May 2015

doi: 10.1109/OCEANS-Genova.2015.7271500

Signal and Receiver Design for Low-Power Acoustic Communications Using M-ary Orthogonal Code Keying

Benjamin Sherlock, Charalampos C. Tsimenidis, Jeffrey A. Neasham
School of Electrical and Electronic Engineering
Newcastle University
Newcastle upon Tyne, NE1 7RU, U.K.
Email: b.sherlock@ncl.ac.uk, charalampos.tsimenidis@ncl.ac.uk, jeff.neasham@ncl.ac.uk

***Abstract*—Low-power, low received signal-to-noise-ratio (SNR) signals have potential for reducing the impact on marine life from acoustic communications. Here we explore the use of bandlimited pseudo-noise m-ary orthogonal code keying (M-OCK) scheme using m-sequences. Analysis and simulation of receiver structure for synchronisation and data demodulation performance is carried out. Performance of M-OCK is compared with m-ary quadrature amplitude modulation with direct-sequence spread-spectrum (M-QAM DSSS). Real-world channel experiments are carried out with transmission power for the M-OCK sequences limited to less than 1 W acoustic power (170.8 dB re 1 µPa at 1 m) and transmission range varied from 100 m to 10 km in the North Sea. Synchronisation at 10 km is achieved with effective received signal-to-noise-ratio of less than -9.96 dB, and data demodulation of 140.7 bit/s raw throughput with pre-coding bit-error-rate (BER) 0.5 X 10-1 (symbol-error-rate (SER) 0.1) and 46.9 bit/s raw throughput with pre-coding BER 0.9 X 10-3 (SER 1.95 X 10-3). Error-free synchronisation and data demodulation is achieved at ranges up to 2 km, demonstrating data rates in excess of 140 bit/s.**

Keywords—underwater acoustic communications; low-power; m-ock; m-ary orthogonal code keying; orthogonal signaling;

I. INTRODUCTION

Research by Dimitrov et al. explored the idea of low-power, low-received-SNR carrierless acoustic communication using pseudo-noise (PN) spreading sequences [1]. The research compares the simulated performance of a BPSK modulated M-Sequence against a carrierless M-Sequence of equal bandwidth-time product. Both the transmit and receive structures of the carrierless system and BPSK modulated system are shown in Fig. 1 and Fig. 2 respectively.

Fig. 3 shows the power spectrum of the carrierless M-Sequence compared to the BPSK modulated M-Sequence. The area of interest is marked by the bandpass limits that show the carrierless signal has a flat spectrum compared to the BPSK modulated signal which possesses a peak at the centre frequency.

The BER and SNR performance of the two systems was compared in simulated ideal AWGN channels [1, Fig. 3]. The carrierless system with BER of 10^{-2} shows a ~4 dB performance gain over the equivalent data rate and bandwidth-time, BPSK modulated M-Sequence scheme.

Sherlock, B.; Tsimenidis, C.C.; Neasham, J.A., "Signal and receiver design for low-power acoustic communications using m-ary orthogonal code keying," in *OCEANS 2015 - Genova* , vol., no., pp.1-10, 18-21 May 2015

doi: 10.1109/OCEANS-Genova.2015.7271500

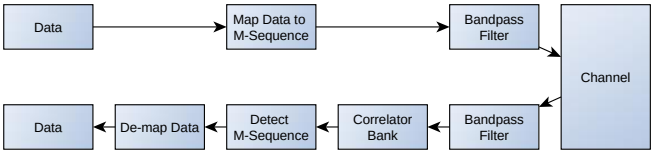

Fig. 1. Block diagram of carrierless system including transmit and receive structures [1, Fig. 1].

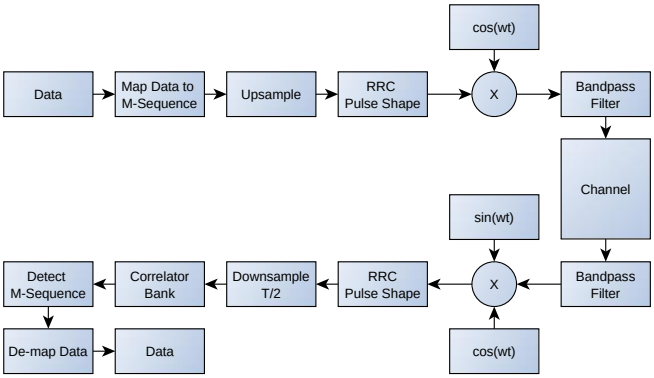

Fig. 2. Block diagram of BPSK modulated system including transmit and receive structures [1, Fig. 2].

There are other approaches to producing low-power, low-received-SNR acoustic communications. Leus and van Walree utilise OFDM to achieve successful communications at 78 bit/s down to a received SNR of -17dB in a benign channel [2]. Research by Ling et al. and, Yang and Yang make use of direct-sequence spread-spectrum signals (DSSS) to provide the necessary process gain for achieving successful communication with low input-SNR signals [3, 4].

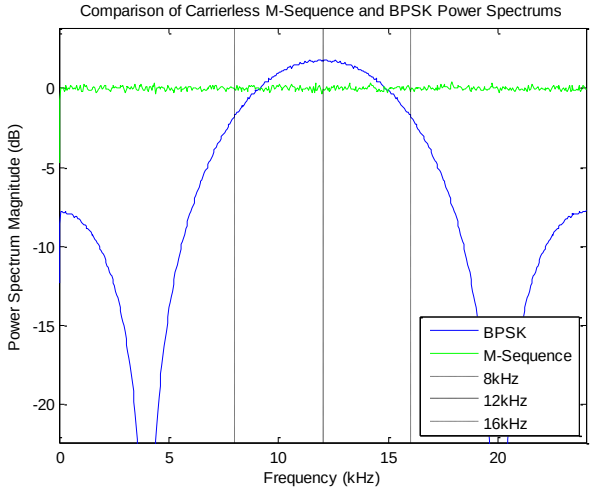

Fig. 3. Power spectrum magnitudes of BPSK modulated M-Sequence and Carrierless M-Sequence signals for sample frequency of 48 kHz. BPSK has a carrier frequency of 12 kHz. The verical lines at 8 kHz and 16 kHz indicate the limits of the bandpass filter of the subsequently transmitted signal.

Sherlock, B.; Tsimenidis, C.C.; Neasham, J.A., "Signal and receiver design for low-power acoustic communications using m-ary orthogonal code keying," in *OCEANS 2015 - Genova* , vol., no., pp.1-10, 18-21 May 2015

doi: 10.1109/OCEANS-Genova.2015.7271500

The carrierless M-Sequence system differs from DSSS. In addition to the absence of a carrier, much longer spreading-sequences are used. Data symbols are based on unique codes, rather than using different codes for multiple access control as in CDMA.

Low-power low-received-SNR underwater acoustic communication systems are potentially useful when considering permanent underwater installations of underwater acoustic transmitters. Distributed networks of battery-powered subsea sensors could allow us to discover, measure and learn so much more of the underwater world. But when studying marine life it is important not to cause negative behavioural effects to the marine life being monitored.

Behavioural responses of marine life have been measured when beaked whales were subjected to mid-frequency SONAR [5] and when tagged blue whales were subjected to simulated mid-frequency military SONAR [6]. In more extreme examples of anthropogenic impact, research by Jepson et al. into the cause of a mass stranding event, involving common dolphins on UK shoreline, points to underwater SONAR transmissions as the most probable cause after ruling out all other possible causes [7].

Marine life in general can be adversely affected by acute or prolonged exposure to underwater acoustic waves. Regulation suggestions include limiting transmission power for communications and SONAR systems. It is expected that as awareness of the environmental impact continues to increase, especially in the public mind, this will lead to governments to legislate in this area [8].

It should be noted that acoustic modem communications tend to use much lower transmit power levels than those used in SONAR applications. However, initial studies have shown behavioural responses of marine life (Harbour Porpoises) to acoustic data emitters centred around 12 kHz [9]. Hearing sensitivities and behavioural responses will vary greatly between different species. Examples of maximum peak exposure levels and sound exposure levels for avoiding sound mediated injury provide a starting point for limiting transmit power [10, Section 10.5.2]. Further exploration into minimising behavioural effects may include location-specific transmit frequency bands and power levels based on known marine populations to target frequencies for which the given marine life share reduced hearing sensitivity.

In an effort to reduce the potential for impact on marine life through acoustic modem transmissions the audible range or “discomfort zone”, in Fig. 4, should be reduced through two approaches:

- increasing the ratio of receivable range to audible range through increased process gain in the signal and receiver design;
- reducing the receivable range by limiting transmitter power for a given configuration such that the receiver lies just within the effective range for successful communication.

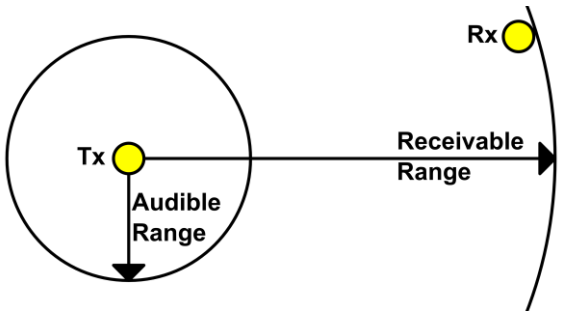

Fig. 4. Comparison of audible and receivable ranges. Transmit power would be reduced to ensure receviable range only just reaches the receiver for a given setup. Signal and receiver design focus on maximising ratio between receivable and audible ranges.

There is a limit to maximising the receivable range to audible range ratio which is defined by the lowest useful target received SNR for a given application.

Using the Shannon-Hartley theorem in (1), we can calculate the channel capacity, *C*, for a given bandwidth, *B*, and signal to noise ratio.

Sherlock, B.; Tsimenidis, C.C.; Neasham, J.A., "Signal and receiver design for low-power acoustic communications using m-ary orthogonal code keying," in *OCEANS 2015 - Genova* , vol., no., pp.1-10, 18-21 May 2015

doi: 10.1109/OCEANS-Genova.2015.7271500

$$C = B\log_2\left(1+\frac{P_{signal}}{P_{noise}}\right) \qquad (1)$$

A bandwidth of 8 kHz targeting a SNR between –15 dB and –20 dB equates to a channel capacity between 359.32 bit/s and 114.84 bit/s respectively.

These data rates would suit applications such as battery-operated sensor networks where telemetry consists of small data packets sent relatively infrequently.

II. Maximal Length Sequences

Maximal Length Sequences, also known as M-Sequences, are a form of pseudo-noise sequence generated by cycling through a linear feedback shift register with a particular configuration of feedback taps. For a given order, or shift register length, of K, this would generate a unique sequence of length $N = 2^K-1$. The feedback tap locations to produce the M-Sequence can be derived from the primitive polynomials for the order, K. Each coefficient is either zero or one and determines the existence of a tap at that position. The shift register can be seeded with any sequence with the exception of all zeros.

M-Sequences have a number of key properties that make them suitable for use in signal spreading:

- They possess a zero D.C. component due to the near balance of zeros and ones. The remaining frequency spectrum is flat with the auto-correlation being delta-like.
- The auto-correlation value of an M-Sequence is equal to its length.
- A number of M-Sequences of a given order possess strong orthogonality when cross-correlated with each other compared to their auto-correlation values.

Code generation using M-Sequences consists of producing a given sequence from a seeded linear feedback shift register and appropriate feedback taps. The sequence is then converted to bipolar non-return-to-zero level (NRZ Level) form at the given sample frequency. This equates to a positive voltage for a binary one or negative voltage for a binary zero value.

Packets are constructed from these codes and then bandpass filtered resulting in a bandlimited pseudo-noise M-ary Orthogonal Code Keying (M-OCK) scheme.

For a given sample frequency of 48kHz and a typical acoustic modem bandwidth of 8kHz we can analyse each set of M-Sequence codes for their auto- and cross-correlation properties in all combinations and lags, spreading process gain, and maximum possible data rates as shown in Table I. This table expands on [11, Table 12.2-1] with additional orders of M-Sequence. Rmax is the peak value at all lags from cross-correlations of all pairs in the code set. R(0) is the peak auto-correlation value for any code within the set. The symbol process gain is the bandwidth-time product using a bandwidth of 8 kHz and a sample frequency of 48 kHz. Knowing the duration of a symbol and the number of codes in a set it is then possible to calculate the maximum data rate with these values.

Challenges of the underwater channel have been widely discussed [12]. Pseudo-noise sequences of the lengths shown here will mismatch rapidly with even a small Doppler shift on the received signal.

The relatively long time duration of these sequences provides an inherent tolerance of multipath delay spread with the subsequent paths arriving within the single symbol duration. This means that this approach does not suffer from Inter-Symbol Interference (ISI). However, there is a limit on maximum code length that can be used due to Doppler spreading and channel coherency time limits.

Sherlock, B.; Tsimenidis, C.C.; Neasham, J.A., "Signal and receiver design for low-power acoustic communications using m-ary orthogonal code keying," in *OCEANS 2015 - Genova* , vol., no., pp.1-10, 18-21 May 2015

doi: 10.1109/OCEANS-Genova.2015.7271500

TABLE I. M-SEQUENCE CODE SET PROPERTIES

Order, K	**Code Set Size**	**Max Data bits / symbol, m**	**Code Length, N=(2^K-1)**	**Rmax / R(0)**	**Symbol Process Gain[b]**	**Max Data bits/s with spreading**
7[a]	18	4	127	0.35	13.26 dB	1511.81
8	16	4	255	0.37	16.28 dB	752.94
9	48	5	511	0.23	19.30 dB	469.67
10	60	5	1023	0.37	22.32 dB	234.60
11	176	7	2047	0.15	25.33 dB	164.14
12	144	7	4095	0.34	28.34 dB	82.05
13[a]	630	9	8191	0.09	31.35 dB	52.74
14	756	9	16383	0.34	34.36 dB	26.37
15	1800	10	32767	0.15	37.37 dB	14.65
16	2048	11	65535	0.34	40.38 dB	8.06

[a] Mersenne Prime.

[b] (Fs=48kHz, W=8kHz)

For the experiments that follow, we will utilise the K11 and K13 code sets due to the relatively low Rmax/R(0) values in Table I. There are other pseudo-noise codes such as Gold codes and Kasami codes, commonly used in CDMA systems due to their ideal periodic cross-correlation properties. It will be worth exploring the suitability of these codes when used in a system such as this. It will also be possible to improve on the M-Sequence code sets by selecting preferential subsets. This is not the focus at this time, but will be worth exploring in more depth in the future.

III. SIGNAL AND RECEIVER DESIGN

Bandlimited PN M-OCK packets are constructed as described in Section II. An individual M-Sequence in this system can be identified by the schema *KxMy* where *Kx* is the order and *My* is the index of the sequence in the code set. For example, *K13M0* would be the first M-Sequence in the code set of length 8191. These identifiers are used for the unique synchronisation headers and also for mapping and de-mapping data to and from symbols in the payload.

With two distinct parts to the transmitted signal packet, the synchronisation header and the data payload, this leads to a receiver structure which also focuses on these elements separately as shown in Fig. 5. Correlating the signal against a given M-Sequence is shared in both parts.

Sherlock, B.; Tsimenidis, C.C.; Neasham, J.A., "Signal and receiver design for low-power acoustic communications using m-ary orthogonal code keying," in *OCEANS 2015 - Genova* , vol., no., pp.1-10, 18-21 May 2015

doi: 10.1109/OCEANS-Genova.2015.7271500

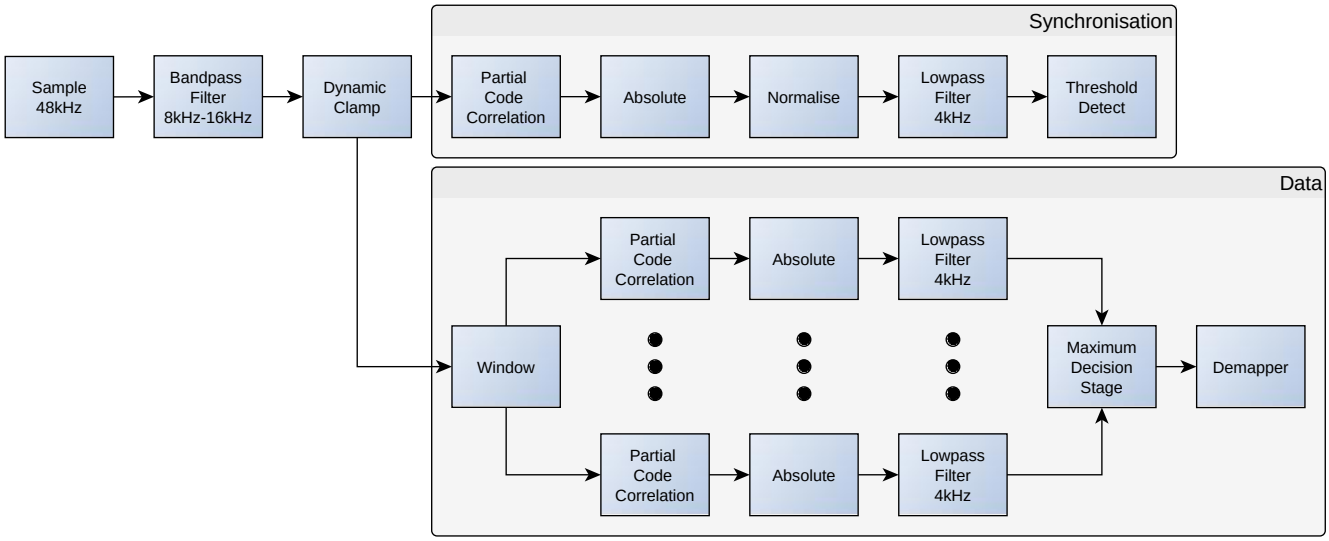

Fig. 5. Block diagram of receiver structure showing the separate synchronisation and demodulation blocks. In the data demodulation the partial code correlation indicates correlating a given code over a windowed input signal. The subsequent lowpass filter reduces the sidelobes and allows the system to trigger or detect on the main lobe.

Reducing the impact of impulsive noise is achieved by dynamically clamping the signal. The signal is hard-limited to a maximum amplitude. If a spike is received the amplitude is limited to this given value. The hard-limit value is altered according to a sliding window RMS of the incoming signal. As the signal rms grows, as will the hard-limit value; and vice versa. It is important to limit the amplitude of such impulsive noise as it can have a negative effect on the subsequent normalisation stages.

The effects of gradually varying signal energy are reduced by using the RMS of a sliding window of the signal after the dynamic clamping stage to normalise the output value of the correlator. Even as the received signal energy varies, the output of the normalised correlator retains a relatively steady noise floor where a fixed threshold value can be used for triggering against in synchronisation. The effects of this can be observed in the experimental results in Section V.

The data demodulator is a maximal likelihood detector with a bank of correlators looking for each code. It is critically important to synchronise successfully so that the maximal likelihood detector is making the comparison at the point of maximum energy on the correlator output. The narrow window for correlation around this point is used to eliminate ISI. This windowing also has the effect of reducing the processing time and energy required by limiting correlation to the narrow windowed input signal rather than continuous correlation over the entire length of the packet. It is possible to counter some of the effects of the Doppler spread on the channel by moving the window after each new data symbol to track the peak energy arrival.

Sherlock, B.; Tsimenidis, C.C.; Neasham, J.A., "Signal and receiver design for low-power acoustic communications using m-ary orthogonal code keying," in *OCEANS 2015 - Genova* , vol., no., pp.1-10, 18-21 May 2015

doi: 10.1109/OCEANS-Genova.2015.7271500

IV. Simulated Receiver Performance

Without successful synchronisation, the data demodulation is not possible. However, successful synchronisation is often the most challenging aspect of communication, and especially so in a system that is targeting a received SNR of less than -15dB in a harsh environment.

A. Synchronisation

Simulating the performance of the synchronisation code in a constant channel, with no multipath, varying the AWGN and a range of threshold values shows the envelope of successful synchronisation for a given M-Sequence as shown in Fig. 6. Too low a threshold value and the system false triggers on noise from the correlator; too high and it becomes impossible to synchronise with low SNR. Comparing two lengths of code it is possible to see the improvement in performance due to the increased process gain from the increase in code duration. However, as the longer codes become more susceptible to channel coherency limits simply increasing the code length used is not an option. It is also possible to use sequential combinations of shorter codes by taking the sum of each code correlation over a narrow window to compensate for channel changes. Fig. 7 compares the performance of a single K14 code with two sequential K13 codes. The performance of the combined K13 symbols should allow us to target a lower received SNR whilst reducing the impact of channel variability.

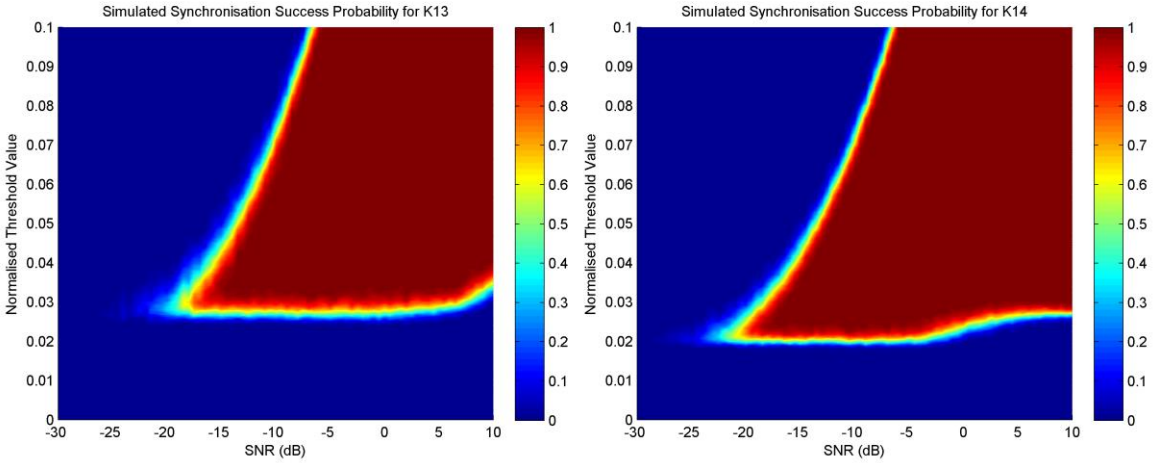

Fig. 6. Simulated synchronisation performance of single K13 and K14 codes in AWGN channel.

Sherlock, B.; Tsimenidis, C.C.; Neasham, J.A., "Signal and receiver design for low-power acoustic communications using m-ary orthogonal code keying," in *OCEANS 2015 - Genova* , vol., no., pp.1-10, 18-21 May 2015

doi: 10.1109/OCEANS-Genova.2015.7271500

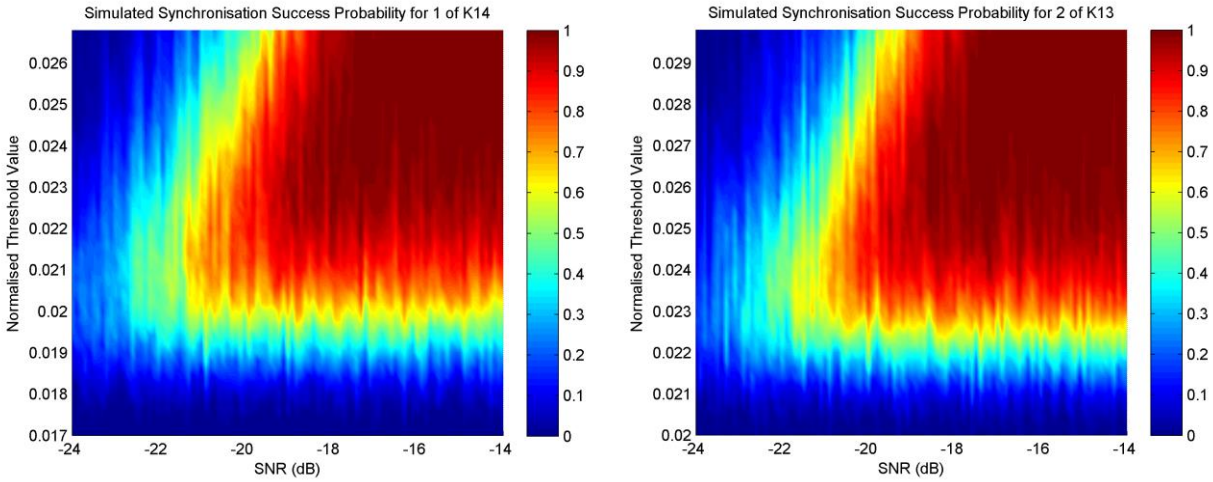

Fig. 7. Simulated synchronisation performance of one K14 code and two K13 codes combined in AWGN channel.

B. Data Demodulation

Successful demodulation using maximal likelihood detection for a given order of M-Sequence can occur at lower SNR values than those required for successful synchronisation. This is without the inclusion of error correction coding which would further improve the performance.

With the larger code set sizes, K13 for instance, the modulation depth possible is around 6 to 8 bits per symbol. Taking into account the process gain from signal spreading it is possible to compare M-OCK with another M-ary system such as M-ary Quadrature Amplitude Modulation with Direct-Sequence Spread-Spectrum (M-QAM DSSS), as shown in Fig. 8.

The strong orthogonality of M-OCK codes means that as the modulation depth is increased for a given symbol size, there is very little degradation in performance. However, as the modulation depth of M-QAM DSSS is increased, the lack of orthogonality means the Euclidean distance between constellation points decreases, resulting in increased bit error rates for a given SNR. Comparing the progression from 16-OCK to 64-OCK and 256-OCK with the progression from 16-QAM DSSS to 64-QAM DSSS and 256-QAM DSSS we see less than 1 dB reduction in performance each time for M-OCK yet a 6 dB reduction in performance each time for M-QAM DSSS at BER of 10^{-4} as shown in Fig. 8.

Sherlock, B.; Tsimenidis, C.C.; Neasham, J.A., "Signal and receiver design for low-power acoustic communications using m-ary orthogonal code keying," in *OCEANS 2015 - Genova* , vol., no., pp.1-10, 18-21 May 2015

doi: 10.1109/OCEANS-Genova.2015.7271500

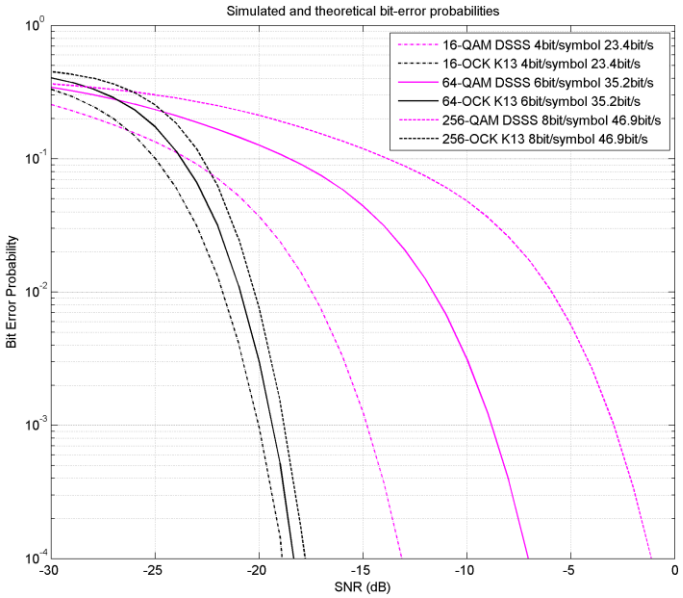

Fig. 8. Simulated and theoretical bit error rate performance of M-QAM DSSS and M-OCK K13 data symbols.

Within the M-Sequence code sets there is a trade-off between processing gain due to the length of code, modulation depth due to the size of the code set, and maximum data rates based on the length of the code and code set size. Comparing 6-bit K11 codes with 8-bit K13 codes shows a three times gain in data rate for a 6 dB reduction in performance as shown in Fig. 9. Optimal data symbol schema will of course depend on the specific application and operating environment requirements.

The analysis of performance characteristics for both synchronisation codes and data codes enables optimal selection of each for a given operating environment when considering the SNR.

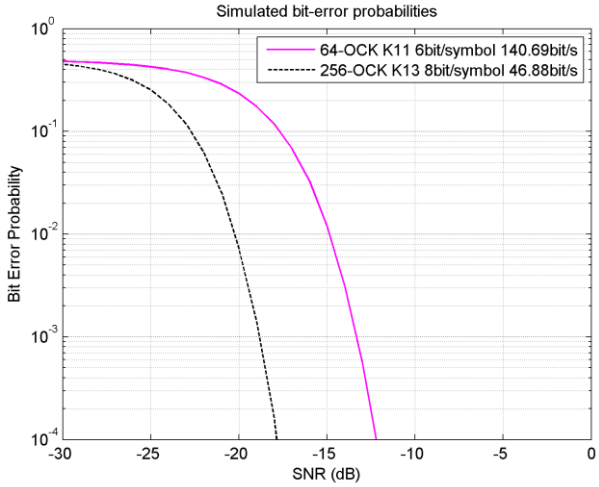

Fig. 9. Simulated bit error rate performance of 64-OCK K11 and 256-OCK K13 data symbols.

Sherlock, B.; Tsimenidis, C.C.; Neasham, J.A., "Signal and receiver design for low-power acoustic communications using m-ary orthogonal code keying," in *OCEANS 2015 - Genova* , vol., no., pp.1-10, 18-21 May 2015

doi: 10.1109/OCEANS-Genova.2015.7271500

V. Experimental Results

The simulations presented in Section IV demonstrate the comparable performance of M-OCK and M-QAM DSSS in idealised AWGN channels. In this section, experimental results highlight the true performance of the proposed scheme, when tested in a real world channel.

A. Experiment Design

M-OCK packets were constructed as shown in Table II including a synchronisation header and data payload.

TABLE II. Packet Structures

Synchronisation Header	Data Symbols	Data bits / symbol	Packet Duration	Data bits/s
K13Ma K13Mb	100 of 64-OCK K11	6	4.61s	140.69
K13Mc K13Md	25 of 256-OCK K13	8	4.61s	46.89

The constructed packets were bandpass filtered to 8kHz-16kHz and written to wave file ready for transmission at 48kHz sample frequency.

The transmitter setup consists of a laptop and soundcard playing the wave file on loop via a power amplifier connected to the transducer. The transducer is suspended at a depth of 20m below the sea surface. The receiver setup consists of a hydrophone, with filtering and amplification, prior to recording using a laptop soundcard to wave file at 48kHz sample frequency. The hydrophone is suspended at a depth of 10m below the sea surface.

Transmission power for the M-OCK sequences was limited to less than 1 W acoustic power (170.8 dB re 1 µPa at 1 m) and the transmission range varied from 100 m to 10 km. Based on the SONAR equations for transmission loss, the expected received SNR at 10 km would in the region of -11 dB.

A 340 ms Linear Chirp was also included at the start of each packet transmission along with a period of silence prior to the M-OCK packets. The transmission level of the linear chirp is 10 dB greater than the M-OCK packet as it is used for the measurement of received SNR.

B. Results and Discussion

Table III and Table IV show the demodulation results for 64-OCK K11 and 256-OCK K13 packets respectively. It is worth noting that the average received SNR values shown here are based on the total received signal energy from all paths and that the receiver structure limits demodulation to the first single path arrival above the synchronisation threshold therefore operating with a lower effective SNR. Both packet types were able to be demodulated error-free up to and including 2 km range.

The channel impulse responses for each distance are shown in Fig. 10 and a variety of multipath examples were encountered. Even in channels with delay spreads containing relatively strong signal paths up to 40 ms (e.g. 100 m and 1 km) the K11 symbols were still able to be demodulated error-free.

Sherlock, B.; Tsimenidis, C.C.; Neasham, J.A., "Signal and receiver design for low-power acoustic communications using m-ary orthogonal code keying," in *OCEANS 2015 - Genova* , vol., no., pp.1-10, 18-21 May 2015

doi: 10.1109/OCEANS-Genova.2015.7271500

TABLE III. 64-OCK K11 DEMODULATION RESULTS

Transmission Range	Average Received SNR	Symbol Count	Symbol Errors	Bit Count	Bit Errors
100 m	12.71 dB	6000	0	36000	0
500 m	11.06 dB	6100	0	36600	0
1 km	8.39 dB	4000	0	24000	0
2 km	9.77 dB	4100	0	24600	0
5 km	-0.56 dB	6000	116	36000	343
10 km	-9.96 dB	4100	410	24600	1199

TABLE IV. 256-OCK K13 DEMODULATION RESULTS

Transmission Range	Average Received SNR	Symbol Count	Symbol Errors	Bit Count	Bit Errors
100 m	12.71 dB	1525	0	12200	0
500 m	11.06 dB	1500	0	12000	0
1 km	8.39 dB	1025	0	8200	0
2 km	9.77 dB	1000	0	8000	0
5 km	-0.56 dB	1525	5	12200	18
10 km	-9.96 dB	1025	2	8200	7

The increase in average received SNR between 1 km and 2 km may be explained by comparing the channel impulse responses for both in Fig. 10. The SNR values were calculated based on all received energy from all paths.

If we look at the bit error rates in Table V for the experimental results we see for 10 km 64-OCK K11 has a BER of 0.487 X 10^{-1} and 256-OCK K13 has a BER of 0.854 X 10^{-3} at SNR below -9.96 dB. Taking into account the effective SNR potentially being below this, based on the simulation results in Fig. 9 we would still expect in an ideal channel to have a BER of less than 10^{-4} for both packet types. This is indicative of the difference between idealised AWGN simulations and experiments in a real-world channel. There is certainly scope for improving these results through Doppler compensation techniques in the receiver structure. There is also potential to exploit the signal energy received via other paths.

TABLE V. DEMODULATION BIT ERROR RATES

Transmission Range	Average Received SNR	64-OCK K11 Bit Error Rate	256-OCK K13 Bit Error Rate
5 km	-0.56 dB	0.953 X 10^{-2}	0.148 X 10^{-2}
10 km	-9.96 dB	0.487 X 10^{-1}	0.854 X 10^{-3}

In the case of the 256-OCK K13, BER performance at 5 km was poorer than at 10 km. As the longer symbols are less tolerant of Doppler shift and channel variation than the shorter K11 symbols, this could suggest greater channel variation and/or relative motion during the recording at the 5 km range.

Sherlock, B.; Tsimenidis, C.C.; Neasham, J.A., "Signal and receiver design for low-power acoustic communications using m-ary orthogonal code keying," in *OCEANS 2015 - Genova* , vol., no., pp.1-10, 18-21 May 2015

doi: 10.1109/OCEANS-Genova.2015.7271500

When considering the symbol error rates at 5 km and 10 km for both K11 and K13 packets, shown in Table VI, it is possible to see that utilising Reed-Solomon error correction coding with a suitable code rate would successfully decode the failed packets. The coding overhead would cause a reduction in data rate for each symbol length, but it is worth exploring whether an error correction coded K11 packet would outperform an uncoded K13 packet in both data rate and performance. As an example, Reed-Solomon error correction coding with a coderate of 0.76 would allow us to correct up to a symbol error rate of 0.12. The effective data rates would then be reduced to 64-OCK K11 106.9 bit/s and 256-OCK K13 35.6 bit/s but if applied to these results would provide error-free communication at these longer ranges even for the shorter K11 symbols. In such a high latency channel, error-free performance is important when considering the time required for re-transmission and the effect on the link data rate.

TABLE VI. DEMODULATION SYMBOL ERROR RATES

Transmission Range	**Average Received SNR**	**64-OCK K11 Symbol Error Rate**	**256-OCK K13 Symbol Error Rate**
5 km	-0.56 dB	19×10^{-3}	3.28×10^{-3}
10 km	-9.96 dB	0.1	1.95×10^{-3}

The performance of the synchronisation as shown in Fig. 11 demonstrates the importance and effectiveness of the normalisation process. At ranges of 100 m and 5 km, over a period of 4 minutes each, the noise floor on the output of the correlator is clearly stable and of the same magnitude. This allows us to set a fixed threshold value for synchronisation at any distance and signal magnitude. As discovered in the simulation results of Fig. 6 it is important that the threshold value is not so low that noise may trigger it, but also that it is not so high that as the received SNR decreases the correlator peaks no longer cross the threshold.

Fig. 12 compares the performance of a single K13 synchronisation code and the combined two K13 synchronisation codes. The correlator values are normalised to the length of the entire synchronisation code length and allow us to compare the noise floor level and peak values. There is an improvement in the ratio of noise floor to peak value, but also importantly it shows that the approach of using multiple codes can be used in a real-world channel. It will be worth exploring this technique further with different code lengths.

The focus on low-power low-received-SNR signals is to drop the signal below the ambient background noise whilst still successfully synchronising and receiving data. Fig. 13 shows the power spectrum of the received ambient background noise compared to the power spectrum of signal combined with the ambient background noise at 10 km.

Sherlock, B.; Tsimenidis, C.C.; Neasham, J.A., "Signal and receiver design for low-power acoustic communications using m-ary orthogonal code keying," in *OCEANS 2015 - Genova* , vol., no., pp.1-10, 18-21 May 2015

doi: 10.1109/OCEANS-Genova.2015.7271500

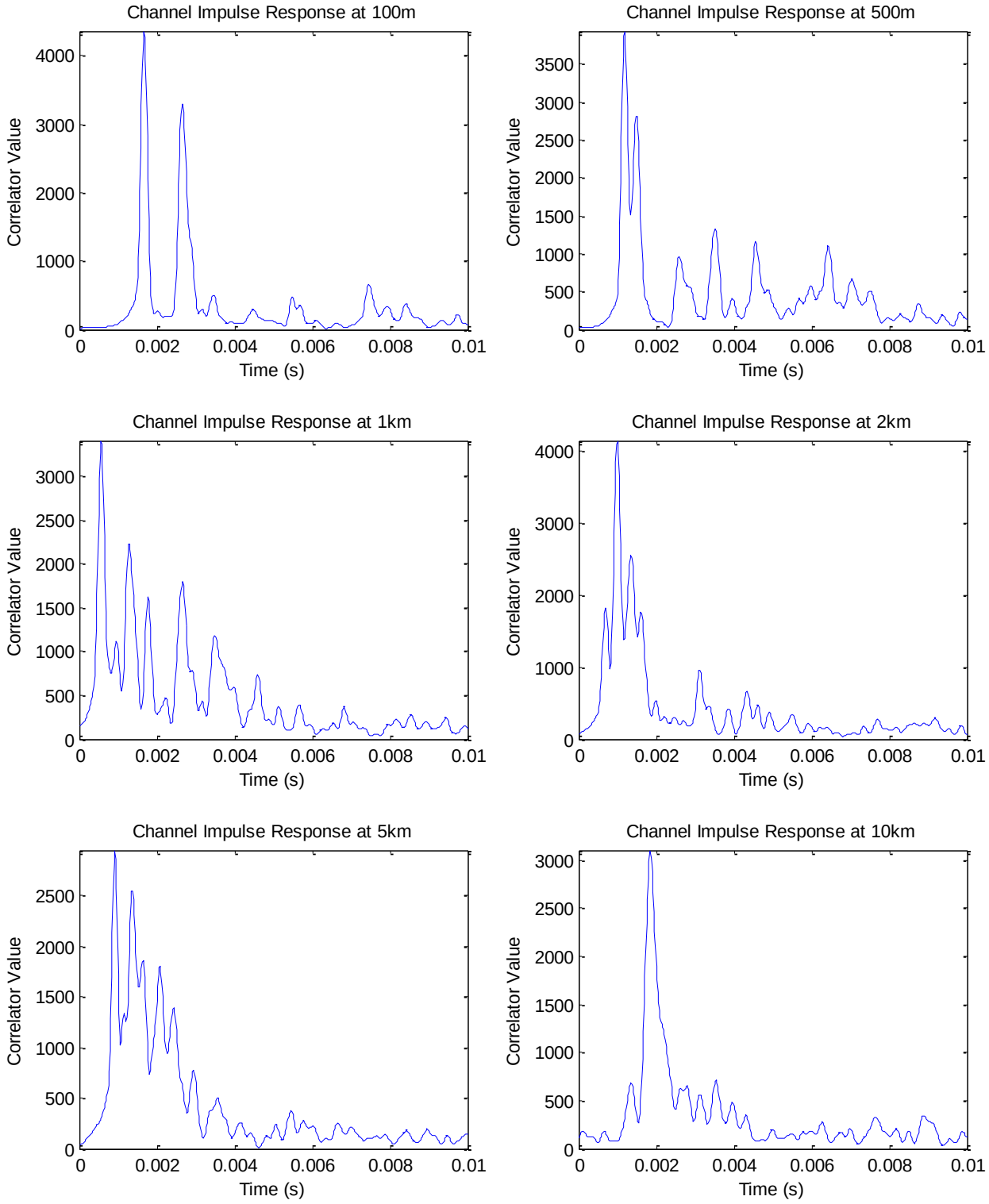

Fig. 10. Channel Impulse Response for each transmission range.

Sherlock, B.; Tsimenidis, C.C.; Neasham, J.A., "Signal and receiver design for low-power acoustic communications using m-ary orthogonal code keying," in *OCEANS 2015 - Genova* , vol., no., pp.1-10, 18-21 May 2015

doi: 10.1109/OCEANS-Genova.2015.7271500

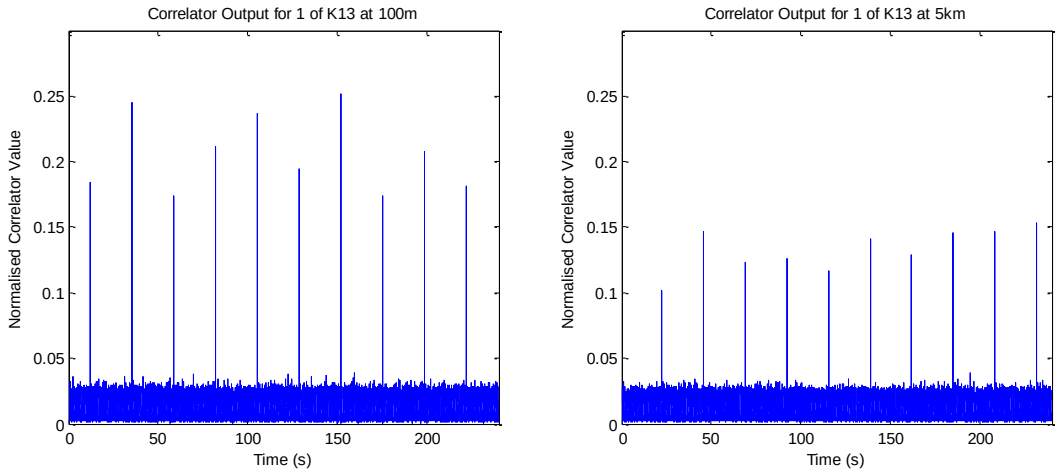

Fig. 11. Normalised correlator output showing similar and stable noise floor at 100m and 5km.

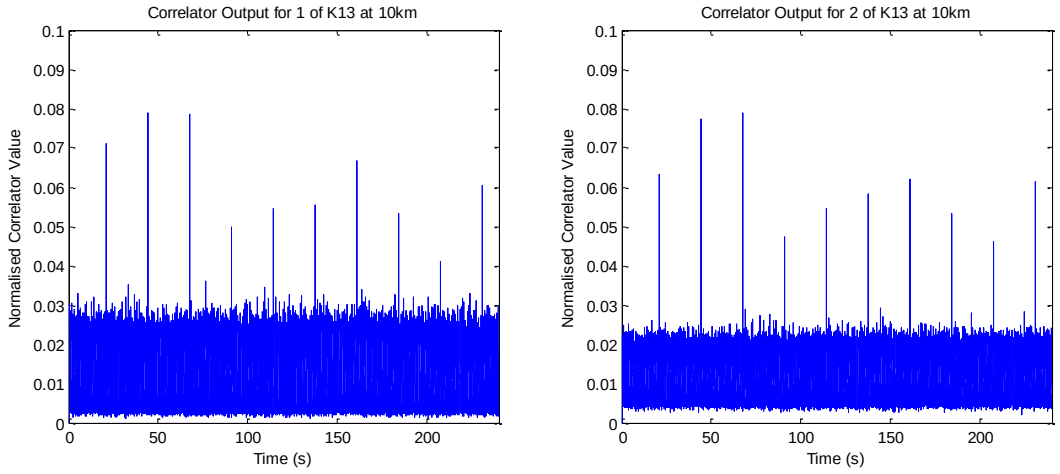

Fig. 12. Normalised correlator output showing improvement when using 2 of K13 instead of 1 of K13 at 10km.

Sherlock, B.; Tsimenidis, C.C.; Neasham, J.A., "Signal and receiver design for low-power acoustic communications using m-ary orthogonal code keying," in *OCEANS 2015 - Genova* , vol., no., pp.1-10, 18-21 May 2015

doi: 10.1109/OCEANS-Genova.2015.7271500

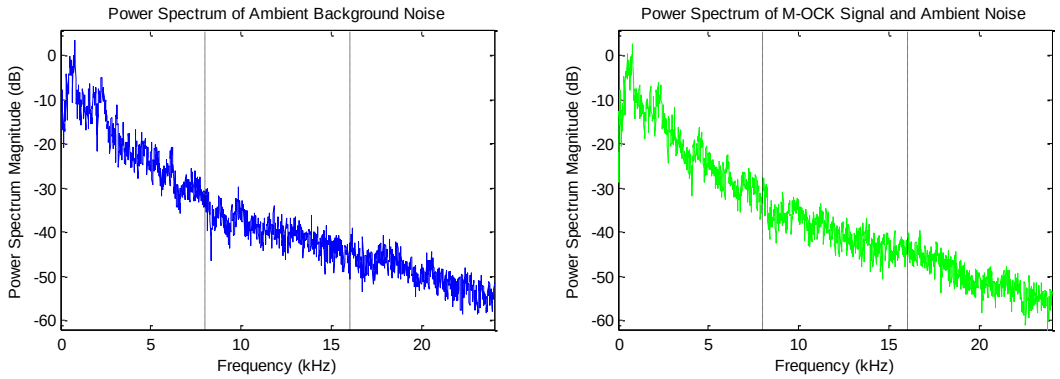

Fig. 13. Power spectrum of the received ambient background noise compared to the power spectrum of signal combined with ambient background noise at 10 km. The vertical lines indicate the 8 kHz to 16 kHz signal spreading bandwidth.

VI. Conclusion

A signal and receiver structure design was considered for low-power acoustic communications using M-ary Orthogonal Code Keying. Simulated performance in idealised AWGN channels showed potential operating limits in the region of -15 dB to -20 dB SNR. Experimental results from real-world channels up to 10 km compared well to the simulations showing successful synchronisation. However, performance of data demodulation BER was considerably less than the simulated AWGN channels. The experiments have demonstrated resilience in the M-OCK scheme to harsh multipath channels at the closer ranges.

The receiver structure, by normalising the correlator output, provides a stable noise floor across a range of received SNR values. This allows us to synchronise successfully using a fixed threshold value for all scenarios. The use of multiple synchronisation codes will allow us to compensate for a changing channel and Doppler spreading whilst retaining increased process gain linked to overall code length.

The strong orthogonality of a code set will allow M-OCK to outperform M-QAM DSSS as the modulation depth increases. Other code sets may allow us to improve on this performance and is certainly worth further work. The longer codes also provide tolerance against ISI in harsh multipath channels.

The data demodulation performance in a real-world channel can potentially be improved on through Doppler compensation techniques in the receiver structure due to the M-Sequences having poor tolerance to Doppler shift. However, even without this, it is possible to improve performance through the use of error correction codes whilst sacrificing data throughput.

Sherlock, B.; Tsimenidis, C.C.; Neasham, J.A., "Signal and receiver design for low-power acoustic communications using m-ary orthogonal code keying," in *OCEANS 2015 - Genova* , vol., no., pp.1-10, 18-21 May 2015

doi: 10.1109/OCEANS-Genova.2015.7271500

ACKNOWLEDGMENT

The authors would like to thank the Newcastle University School of Marine Science and Technology for the use of the RV Princess Royal and the SEAlab team for their assistance during the sea trials.

REFERENCES

[1] K. E. Dimitrov, J. A. Neasham, B. S. Sharif, C. C. Tsimenidis, G. M. Goodfellow, “Low-power environmentally friendly underwater acoustic communication using pseudo-noise spreading sequences,” OCEANS, 2012 - Yeosu, 2012, pp. 1–5.

[2] G. Leus, P. A. van Walree, “Multiband OFDM for covert acoustic communications,” Selected Areas in Communications, IEEE Journal on, vol. 26, no. 9, 2008.

[3] J. Ling, H. He, J. Li, W. Roberts, P. Stoica, “Covert underwater acoustic communications,” J. Acoustical Society of America, vol. 128, pp. 2898-2909, 2010.

[4] T.C. Yang, W. B. Yang, “Performance analysis of direct-sequence spread-spectrum underwater acoustic communications with low signal-to-noise-ratio input signals,” J. Acoustical Society of America, vol. 123, pp. 842-855, 2008.

[5] S. L. DeRuiter et al. “First direct measurements of behavioural responses by cuvier’s beaked whales to mid-frequency active sonar,” Biology Letters, vol. 9, no. 4, 2013.

[6] J. A. Goldbogen et al. “Blue whales respond to simulated mid-frequency military sonar,” Proceedings of the Royal Society B: Biological Sciences, vol. 280, no. 1765, 2013.

[7] P. D. Jepson et al. “What caused the UK’s largest common dolphin (delphinus delphis) mass stranding event?” PLoS ONE, vol. 8, no. 4, p. e60953, 04 2013.

[8] T. Goetz et al. “Overview of the impacts of anthropogenic underwater sound in the marine environment,” OSPAR BioDiversity Series, vol. 441, 2009.

[9] R. A. Kastelein, W. C. Verboom, M. Muijsers, N. V. Jennings, S. van der Heul, “The influence of acoustic emissions for underwater data transmission on the behaviour of harbour porpoises (phocoena phocoena) in a floating pen,” Marine Environmental Research, vol. 59, No. 4, pp. 287-307, 2005.

[10] X. Lurton, “An introduction to underwater acoustics: principles and applications, 2nd ed.,” Springer-Praxis, 2010.

[11] J. G. Proakis, M. Salehi, “Digital communications, 5th ed.,” New York : McGraw-Hill Higher Education, 2008.

[12] M. Stojanovic, "Underwater acoustic communications: design considerations on the physical layer," Wireless on Demand Network Systems and Services, 2008. WONS 2008. Fifth Annual Conference on , pp.1,10, 23-25 Jan. 2008.